IX. ELECTRODYNAMICS OF MEDIA

Academic Research Staff

Prof. Hermann A. Haus   Prof. Paul L. Penfield, Jr.
Prof. Jin-Au Kong   Prof. David H. Staelin

Graduate Students

Zemen Lebne-Dengel
Eni G. Njoku
Leung Tsang

A. EFFECT OF SURFACE ROUGHNESS ON EMISSIVITY

With a radiometer looking directly downward at a rough surface, after integration over $d\theta_s$, the emissivity of the surface[1] is given by

$$e = 1 - \frac{1}{4\pi} \int \gamma(0, \bar{k}_s) \sin \theta_s \, d\theta_s, \tag{1}$$

where

$$\gamma(0, \bar{k}_s) = \frac{k^2 |f|^2}{2} I \tag{2}$$

is the scattering cross section for a wave at normal incidence, and $\bar{k}_s$ is the scattering $\bar{k}$-vector. In Eq. 2, $|f|^2 = 2\pi(2 \sin^2 \theta_s + 2 |R_{01}|^2 - |R_{01}|^2 \sin^2 \theta_s - 2 \cos \theta_s + 2 |R_{01}|^2 \cos \theta_s)$ and

$$I = \int_0^\infty \xi J_0(k_{d\rho}\xi) \, e^{-\kappa(1-\rho(\xi))} \, d\xi, \tag{3}$$

where $\rho(\xi)$ is the surface height correlation coefficient, and $\kappa = (k_{sz}+k_o)^2 \sigma^2$, with σ the root mean height of the surface. The z axis is normal to the surface when it is flat and $k_{d\rho}$ and k_{dz} denote the horizontal and vertical components of $\bar{k}_d = \bar{k}_s - \bar{k}_i$, where k_i is the incident wave vector.

The solution to the integral I in (3) has been a controversial subject.[2,3] In this report, we use the double saddle-point method to evaluate I. The integral is extended to the complex plane[4]

$$I = \frac{1}{2} \int_{-\infty}^{\infty} \xi H_0^{(1)}\left(k_{d\rho}\xi\right) e^{-\kappa(1-\rho(\xi))} \, d\xi$$

$$= \frac{2}{\pi} \int_{-\infty}^{\infty} \xi e^{ik_{d\rho}\xi} e^{-\kappa(1-\rho(\xi))} \, d\xi \int_0^{\infty} \left(i4k_{d\rho}\xi - y^2\right)^{-1/2} e^{-y^2/2} \, dy. \tag{4}$$

Assuming a Gaussian correlation function

$$\rho(\xi) = \exp(-\xi^2/L^2), \tag{5}$$

where L is the correlation length, we determine the saddle point ξ_s from

$$\xi_s \exp\left(-\xi_s^2/L^2\right) = ik_{d\rho}L^2/2\kappa \tag{6}$$

and it is found to be on the imaginary axis. Applying the transformation

$$ik_{d\rho}\xi - \kappa(1-\rho(\xi)) - \left[ik_{d\rho}\xi_s - \kappa(1-\rho(\xi_s))\right] = -s^2/2,$$

we can expand the integrand into a double power series of s and y. The result of the integration is an asymptotic series, which to second order is

$$I = \left(\frac{\xi_s}{ik_{d\rho}}\right)^{1/2} \exp(-\kappa(1-\rho(\xi_s)) + ik_{d\rho}\xi_s)\left(\frac{L^2 \exp\left(\xi_s^2/L^2\right)}{2\kappa\left(1-2\xi_s^2/L^2\right)}\right)^{1/2}$$

$$\left\{1 + \frac{\exp\left(\xi_s^2/L^2\right)}{4\kappa\left(1 - \frac{2\xi_s^2}{L^2}\right)^3}\left[1 - \frac{12\xi_s^2}{L^2} + \frac{8\xi_s^4}{L^4} - \frac{8\xi_s^6}{L^6}\right]\right\}. \tag{7}$$

In the limit $\xi_s \ll L$, Eq. 6 becomes

$$\xi_s \approx ik_{d\rho}L^2/2\kappa, \tag{8}$$

and Eq. 7 becomes

$$I = \frac{L^2}{2\kappa} e^{-k_{d\rho}^2 L^2/4\kappa}\left\{1 + \frac{1}{4\kappa} - \frac{3k_{d\rho}^2 L^2}{8\kappa^2} + \frac{k_{d\rho}^4 L^4}{32\kappa^3}\right\} \tag{9}$$

The first term in (9) is the solution from geometrical optics.[5]

In order to calculate emissivity, another integration must be performed. We can apply the saddle-point method with the saddle point at $\theta_s = 0$ and obtain

$$e = 1 - |R_{01}|^2 \left(1 - \frac{16}{3} \frac{\sigma^2}{L^2} - \frac{1}{16k^2\sigma^2}\right) \tag{10}$$

The approximation $\xi_s \ll L$ leading to (8), in view of (6), implies $1 \gg \sigma^2/L^2 \gg 1/k^2\sigma^2$. Thus in Eq. 10 the last term is negligible. The scattering effect reduces the reflectivity and consequently increases the emissivity. In view of the last term, the emissivity decreases as frequency increases.

In the limit $k\sigma \ll 1 \ll kL$, this method breaks down and our results are invalid. In this limit we can follow Stogryn's small-perturbation approach,[6] which utilizes the bistatic scattering cross-section results of Rice[7] and Valenzuela,[8] and obtain

$$e = 1 - |R_{01}|^2 \left(1 + 4k^2\sigma^2 + 2k^2\sigma^2(n-1)(1+R_{01})/|R_{01}|\right). \tag{11}$$

Thus the scattering effect increases the reflectivity and consequently decreases the emissivity. The emissivity decreases as frequency increases.

References

1. W. H. Peake, "Interaction of Electromagnetic Waves with Some Natural Surfaces," IRE Trans., Vol. AP-7, Special Supplement, pp. S324-S329, December 1959.

2. A. K. Fung and A. Leovaris, "Experimental Verification of the Proper Kirchhoff Theory of Wave Scattering from Known Randomly Rough Surfaces," J. Acoust. Soc. Am. 46, 1057 (1969).

3. W. H. Peake, D. L. Barrick, A. K. Fung, and H. L. Chan, "Comments on 'Backscattering of Waves by Composite Rough Surfaces'," IEEE Trans., Vol. AP-18, No. 5, pp. 716-726, September 1970.

4. A. Banos, Dipole Radiation in the Presence of Conducting Half Space (Pergamon Press, New York, 1966).

5. F. T. Ulaby, A. K. Fund, and S. Wu, "The Apparent Temperature and Emissivity of Natural Surfaces at Microwave Frequencies," Technical Report 133-12, University of Kansas, Lawrence, Kansas, March 1970.

6. G. Poe, A. Stogryn, and A. T. Edgerton, "A Study of the Microwave Emission Characteristics of Sea Ice," Report 1749 R-2, Aerojet Electrosystems Company, Azusa, California, September 1972.

7. S. Rice, "Reflection of Electromagnetic Waves from Slightly Rough Surfaces," Communs. Pure Appl. Math. 4, 351 (1951).

8. G. R. Valenzuela, "Depolarization of EM Waves by Slightly Rough Surfaces," IEEE Trans., Vol. AP-15, No. 4, pp. 552-557, July 1967.

B. COMPOSITE MODEL FOR MICROWAVE REMOTE SENSING

California Institute of Technology (Contract 953524)

Jin-Au Kong

In microwave remote sensing of the Earth, the factors that affect emission properties include absorption, layering, surface roughness, anisotropy, inhomogeneities, and scattering. No model that takes into account only individual factors can interpret actual field data because the data are affected by all of the factors. In this report, we attempt to develop a composite model that accomodates all of these effects.

We use as our starting point a stratified model,[1] which has been developed to account for absorption, layering, and anisotropy. The solution is exact and in closed form. We propose that the reflectivity at each interface in the solution be modified to include rough surface effects as discussed in Section IX-A. The effects attributable to buried scattering centers can be treated separately and subtracted from the resultant emissivity.

As an example to illustrate the procedure, we consider a two-layer model such as a slab of ice with depth d and relative complex permittivity $\epsilon'_1 + i\epsilon''_1$ on top of water or land. We calculate emissivity as a function of frequency. The reflection coefficient is

$$R = \frac{R_{01} + R_{12} \exp(i2k_{1x}d)}{1 + R_{01}R_{12} \exp(i2k_{1x}d)} \quad , \tag{1}$$

where R_{01} is the reflection coefficient at the air-ice boundary, R_{12} is the reflection coefficient at the ice-water or the ice-land boundary, and $k_{1x} = k_o(\epsilon'_1 + i\epsilon''_1 - \sin^2\theta)^{1/2} = k'_{1x} + ik''_{1x}$, where θ is the angle of observation measured from the nadir.

The reflectivity $r = |R|^2$ is calculated as

$$r \approx \frac{A^2 + |R_{01}|^2}{1 + A^2 |R_{01}|^2}, \tag{2}$$

where

$$A = |R_{12}| \exp(-2k''_{1x}d). \tag{3}$$

In arriving at (2), we have neglected the oscillatory behavior of r with frequency because scattering and inhomogeneity will render the wave incoherent. We observe that absorption is accounted for by A, which becomes small for large layer depth or highly lossy
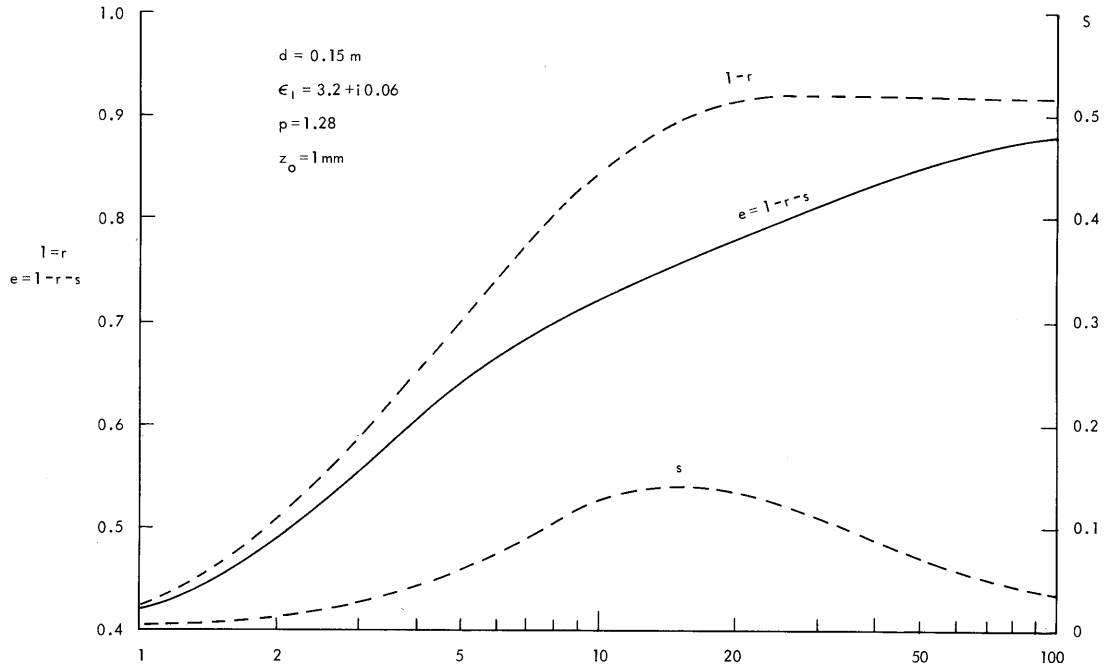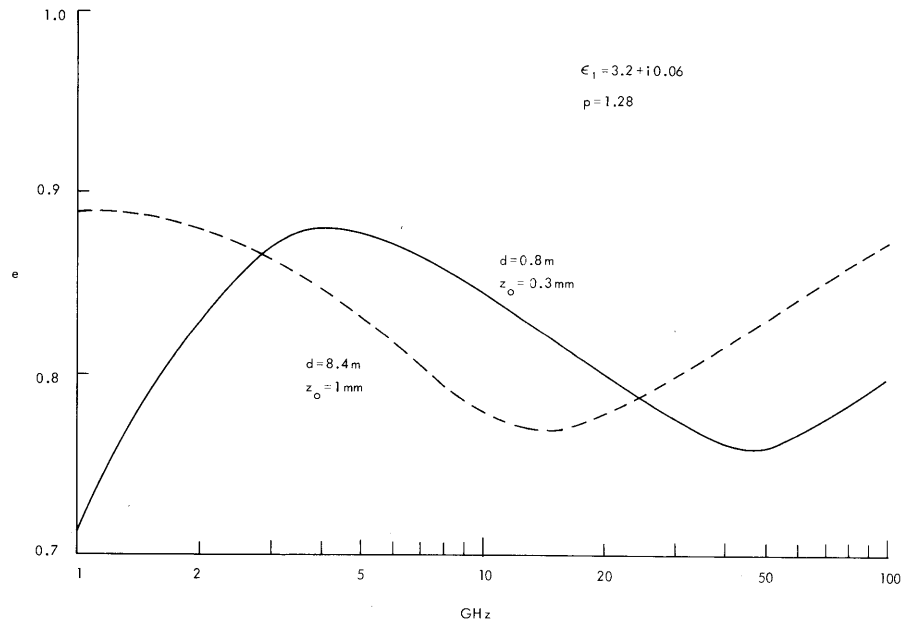
Fig. IX-1. Emissivity with and without scattering.

Fig. IX-2. Emissivities.

ice, and $r \approx |R_{01}|^2$. When the interfaces are not flat, we take into account rough surface effects by modifying $|R_{01}|^2$ and $|R_{12}|^2$ according to Eqs. 10 and 11 in Section IX-A.

We treat scattering effects arising from medium inhomogeneity by extending Gurvich's result[2] for an unbounded half space. Assuming scattering is caused only by ice because the penetration depth for water or land is vanishingly small, we obtain

$$s = \frac{n}{2n_i} \sigma_{no}^2 \frac{nk_o z_o}{1 + 4(nk_o z_o)^2} \left(1 - |R_{01}|^2\right)(1 - \exp(-4n_i k_o d)), \tag{4}$$

where $n + in_i$ is the complex refractive index for ice, z_o is the characteristic correlation depth for the refractive index, and σ_{no}^2 characterizes the variance of the refractive index. Equation 4 is valid only for observation from the nadir and the last factor accounts for the finite depth of ice.

The emissivity with all effects present is given by

$$e = 1 - r - s. \tag{5}$$

Neglecting the rough surface effect and observing from the nadir, we find that e is governed by $n + in_i = (\epsilon_1' + i\epsilon_1'')^{1/2}$, d, z_o, and $p = \sigma_{no}^2(n/n_i)$. In Fig. IX-1, we present a numerical result for s, $1-r$, and e. The Lorentzian-shaped s has its maximum point shifted toward the higher frequency side when z_o decreases, and the magnitude of the maximum point increases as p increases. In Fig. IX-2, we show emissivities for two sets of different parameters.

I am indebted to Dr. Joe W. Waters for bringing to my attention Gurvich's paper and to Leung Tsang for his perceptive views toward this work and many illuminating discussions.

References

1. J. A. Kong, "Electromagnetic Waves in Layered Biaxial Media," Quarterly Progress Report No. 110, Research Laboratory of Electronics, M.I.T., July 15, 1973, pp. 34-38.

2. A. S. Gurvich, V. I. Kalinin, and D. T. Matmeyer, "Relation of the Internal Structure of Glaciers to Their Thermal Radioemission," Atmos. Phys. 9, 1247-1255 (1973).

C. PROBING DEPTH FOR MICROWAVE REMOTE SENSING OF
   ICE AND SNOW CALCULATED BY A SEMINUMERICAL
   APPROACH USING MACSYMA

California Institute of Technology (Contract 953524)

Jin-Au Kong

In microwave remote sensing of snow and ice fields, we are especially interested in the penetration depth. A simple layer model was used and with the aid of MACSYMA we quickly obtained a closed-form solution for the probing depth (see the appendix). The radiometer sensitivity is assumed to be accurate within 1%.

For a layer of ice with relative dielectric constant $\epsilon = 3.2 + i\epsilon''$ on top of water, the probing depths are as follows.

For lake ice with $\epsilon'' = 0.004$, dp = 255λ.

For sea ice with $\epsilon'' = 0.2$, dp = 5.1λ.

For glacier ice with $\epsilon'' = 6.14 \times 10^{-4}/\lambda$, dp = 1660$\lambda$.

(λ is the free-space wavelength in meters.)

I wish to thank Professors J. Moses and A. Bers for giving me access to their facilities, and Dr. David Yun, Charles Karney, and John Kulp for teaching me MACSYMA.

Appendix

```
THIS IS MACSYMA 244

FIX 244 DSK MACSYM BEING LOADED
LOADING DONE

(C1) batch(probing,depth);

(C2) T:2$

(C3) LINEL:73$

(C4) D[0]:0$

(C5) D[T]:0$

(C6) REF[T]:0$

(C7) FOR L:T-1 THRU 0 STEP -1
DO REF[L]:1/R[L,L+1]+(1-1/R[L,L+1]**2)*EXP(-%I*2*KX[L+1]*(D[L+1]-D[L]))
/(EXP(-%I*2*KX[L+1]*(D[L+1]-D[L]))/R[L,L+1]+REF[L+1])$

(C8) R2:RATSIMP(REF[0]);
```

$$
(D8) \qquad \frac{\%E^{2\%I\,D_1\,KX_1}\,R_{1,2} + R_{0,1}}{R_{0,1}\,\%E^{2\%I\,D_1\,KX_1}\,R_{1,2} + 1}
$$

```
(C9).MATCHDECLARE(A,TRUE)$

MATCOM FASL DSK MACSYM BEING LOADED
LOADING DONE

(C10) TELLSIMP(SIN(A)**2,1-COS(A)**2)$
RULE PLACED ON **

(C11) KX[1]:KP+%I*KPP$

(C12) R2:EV(R2);
```
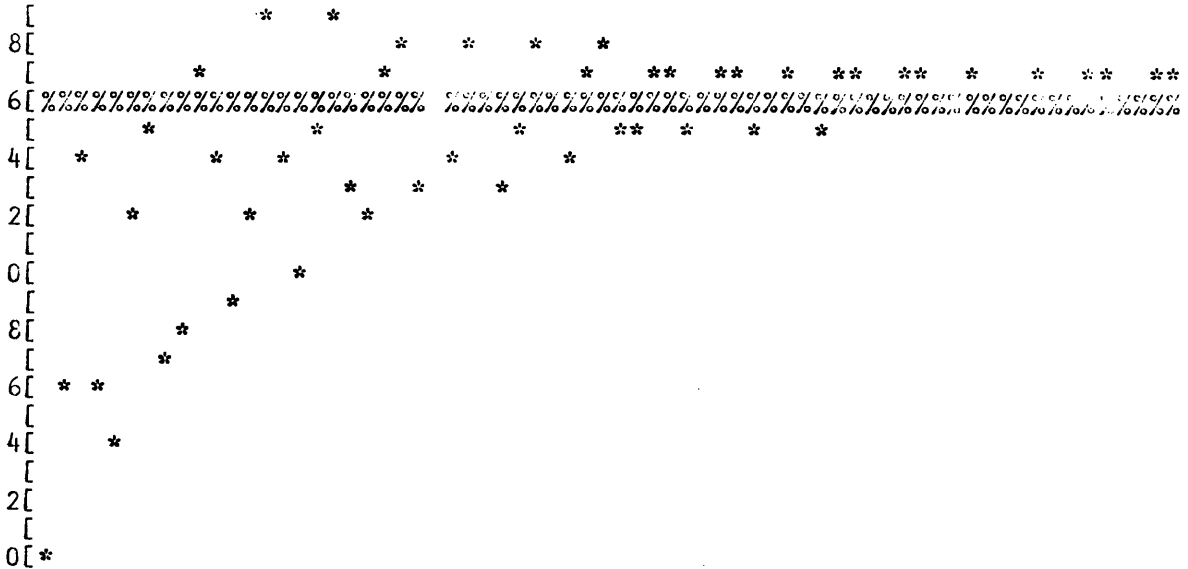
$$
(D12) \qquad \frac{R_{1,2}\,\%E^{2\%I\,D_1\,(\%I\,KPP + KP)} + R_{0,1}}{R_{0,1}\,R_{1,2}\,\%E^{2\%I\,D_1\,(\%I\,KPP + KP)} + 1}
$$

```
(C13)  PN:PART(R2,1)$

(C14)  PD:PART(R2,2)$

(C15)  PR:(REALPART(PN)**2+IMAGPART(PN)**2)
       /(REALPART(PD)**2+IMAGPART(PD)**2)$

(C16)  KP:SQRT(3.2)$

(C17)  KPP:SQRT(.0032)$

(C18)  R[0,1]:(1-SQRT(3.2))/(1+SQRT(3.2))$

(C19)  R[1,2]:(1-SQRT(80/3.2))/(1+SQRT(80/3.2))$

(C20)  PLOT([1-R[0,1]**2,1-PR],D[1],0,10*%PI,[%]);
```

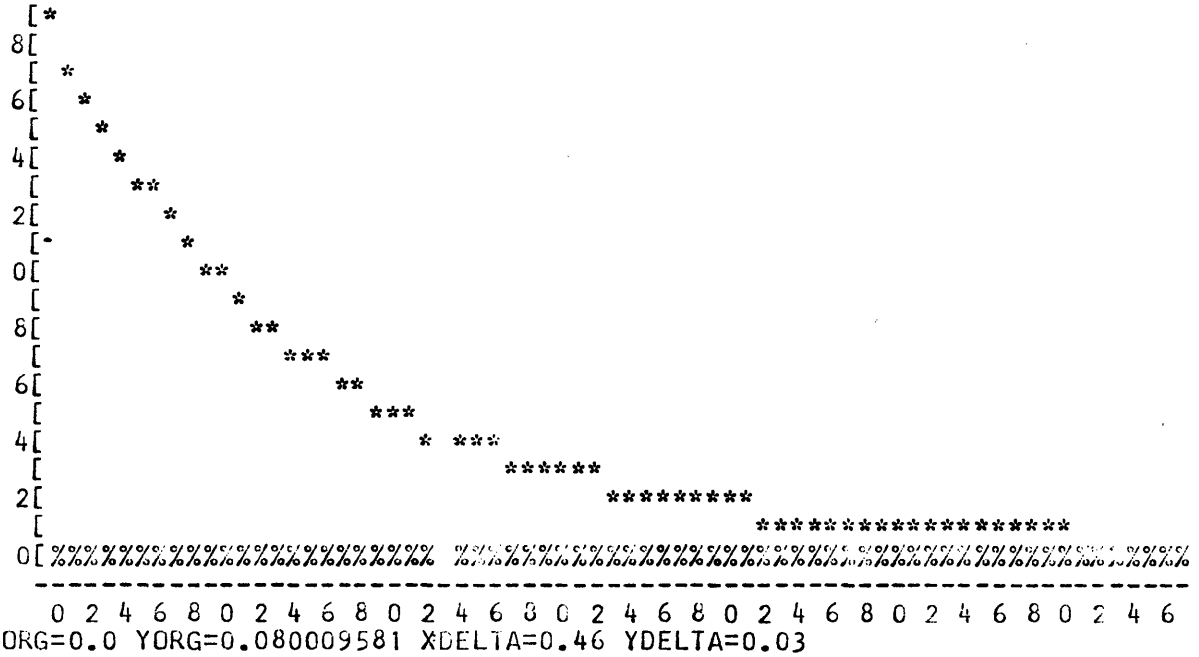GRAPH FASL DSK MACSYM BEING LOADED
LOADING DONE


```
XORG=0.0 YORG=0.36179204 XDELTA=0.46 YDELTA=0.034
```

(D20)   DONE

(C21) KP:0$

(C22) PLOT([R[0,1]**2,PR],D[1],0,10*%PI,[%]);

```
    [*
  8[
   [   *
  6[    *
   [     *
  4[      *
   [       **
  2[        *
   [-         *
  0[          **
   [           *
  8[            **
   [             ***
  6[              **
   [               ***
  4[                *  ***
   [                  ******
  2[                       *********
   [                           ****************************
  0[%%%%%%%%%%%%%%%%%%%%%%%%%% %%%%%%%%%%%%%%%%%%%%%%%%%%%%%%%%%%%%%%%%%%%%%%
   ------------------------------------------------------------------------
     0 2 4 6 8 0 2 4 6 8 0 2 4 6 8 0 2 4 6 8 0 2 4 6 8 0 2 4 6 8 0 2 4 6
XORG=0.0 YORG=0.080009581 XDELTA=0.46 YDELTA=0.03
```

(D22)   DONE

(C23) KILL(R[0,1],R[1,2],KPP)$

(C24) PR:EV(PR);

$$
(D24) \qquad \frac{(R_{1,2}\, \%E^{-2\,D_1\,KPP} + R_{0,1})^2}{(R_{0,1}\, R_{1,2}\, \%E^{-2\,D_1\,KPP} + 1)^2}
$$

(C25) EQ:RATSUBST(X,EXP(-2*D[1]*KPP),PR-R[0,1]**2=DEL);

$$
(D25) \quad -\frac{R_{1,2}^2\,(R_{0,1}^4\,X^2 - X^2) + R_{1,2}\,(2\,R_{0,1}^2\,X - 2\,R_{0,1}^3\,X)}{R_{0,1}^2\,R_{1,2}^2\,X^2 + 2\,R_{0,1}\,R_{1,2}\,X + 1} = DEL
$$

(C26) SOL:SOLVE(EQ,X);
SOLUTION

$$(E26) \quad X = - \frac{(R_{0,1}^2 - 1) \, SQRT(DEL + R_{0,1}^2) + R_{0,1} \, DEL + R_{0,1}^3 - R}{R_{1,2} \, (R_{0,1}^2 \, DEL + R_{0,1}^4 - 1)}$$

$$(E27) \quad X = - \frac{(1 - R_{0,1}^2) \, SQRT(DEL + R_{0,1}^2) + R_{0,1} \, DEL + R_{0,1}^3 - R}{R_{1,2} \, (R_{0,1}^2 \, DEL + R_{0,1}^4 - 1)}$$

(D2)   [E26, E27]

(C28) SOL:EV(SOL)$

(C29) R[0,1]:ABS((1-SQRT(3.2))/(1+SQRT(3.2)));
(D29)   0.28285965

(C30) R[1,2]:ABS((1-SQRT(80/3.2))/(1+SQRT(80/3.2)));
(D30)   0.66666666

(C31) DEL:.01$

(C32) SOL:EV(SOL);
(D32)   [X = - 0.80592103, X = 0.028120892335]

(C33) LOG(X),EVAL,SOL[2];
(D33)   - 3.5712425

(C34) DP:-%/(2*KPP)$

(C35) KPP:(EPP/SQRT(EP))*%PI/LAMDA$

(C36) DP:EV(DP,NUMER);

$$(D36) \quad \frac{1.78562124 \, EP^{0.5} \, LAMDA}{\%PI \, EPP}$$

(C37) EP:3.2$

(C38) DP1:EV(DP,EPP=.01*EP,NUMER);
(D38)   31.7734585 LAMDA

(C39) DP2:EV(DP,EPP=.0004*EP,NUMER);
(D39)   794.33646 LAMDA

(C40) DP3:EV(DP,EPP=.000192*EP/LAMDA,NUMER);

$$(D40) \quad 1654.86766 \, LAMDA^2$$

(D41)   BATCH DONE

JS

D. MACSYMA STUDIES OF WAVES IN UNIAXIAL MEDIA

Joint Services Electronics Program (Contract DAAB07-71-C-0300)

Zemen Lebne-Dengel, Eni G. Njoku, Jin-Au Kong

By using the symbolic manipulation program MACSYMA, waves in uniaxial media have been studied analytically and numerically. In this report we summarize results that have not been reported elsewhere.

Case 1: We studied waves in a uniaxial medium that moves in a direction perpendicular to the optical axis. The dispersion relation is derived by using a Lorentz transformation or the kDB system. For extraordinary waves, the result is

$$k_y^2 + ak_z^2 + \frac{1 - an^2\beta^2}{1 - \beta^2}\left[k_x + \beta\frac{an^2 - 1}{1 - an^2\beta^2}\frac{\omega}{c}\right]^2 - \frac{an^2}{1 - an^2\beta^2}\frac{\omega^2}{c^2} = 0,$$

where k_x, k_y, and k_z are the three components of the wave vector, $\beta = v/c$ determines the velocity of the medium, ω is the angular frequency, n is the refractive index in
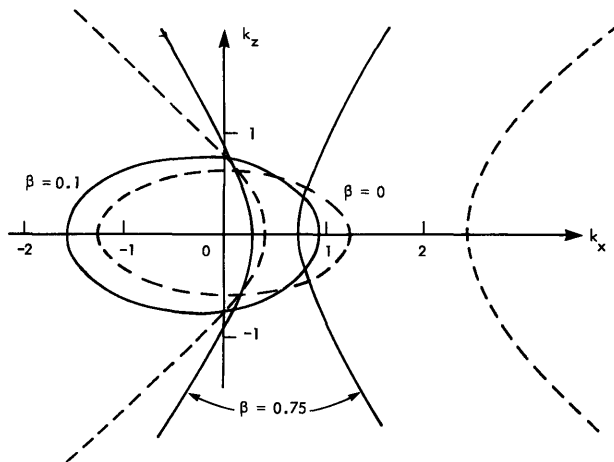

Fig. IX-3.
Wave surfaces for a moving uniaxial medium.

the rest frame of the medium, and a characterizes the anisotropy (for a positive uniaxial medium a > 1, for a negative uniaxial medium a < 1). In Fig. IX-3, we plot the wave surfaces in the k_x and k_z planes at different velocities. Since $\beta = 0$, we obtain the usual ellipse. The ellipse is shifted to the left as the velocity increases, which indicates that the wave velocity decreases in the direction of motion of the medium. Since the velocity of the medium exceeds Čerenkov velocity $\beta = 1/n$, the wave surfaces become hyberbolas.

JS

Case 2: We studied the reflections of a plane wave incident upon a stationary

uniaxial medium. The optical axis of the uniaxial medium is oriented in an arbitrary   JS
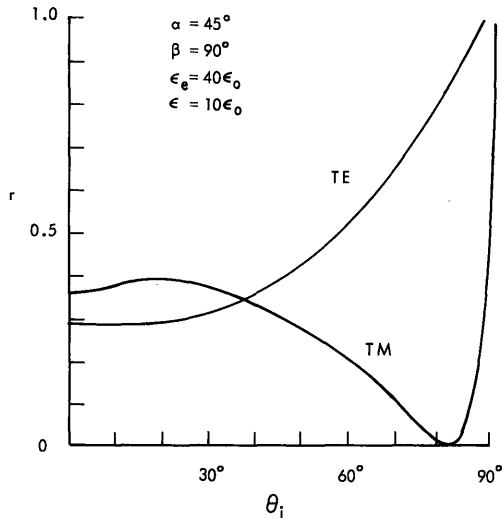direction.   In Fig. IX-4 we present the reflectivity for both TE and TM incident

$\alpha = 45°$
$\beta = 90°$
$\epsilon_e = 40\epsilon_0$
$\epsilon = 10\epsilon_0$

Fig. IX-4. Reflectivity of TE and TM waves from
a uniaxial medium.

waves as a function of incident angle θ_i.   The optical axis in this case is oriented 45°
with respect to normal and lies in the plane of incidence. The crossover of the two
curves occurs because for the incident TE wave only the ordinary wave is transmitted,
while for the incident TM wave only the extraordinary wave is transmitted.

E.   APPLICATION OF THE RADIO-FREQUENCY INTERFEROMETRY
     METHOD TO STRATIFIED ANISOTROPIC EARTH

Leung Tsang, Jin-Au Kong

In previous publications,[1-3] we determined interference patterns produced by a
horizontal electric dipole laid on the surface of a stratified isotropic medium.   Other
work in the past has been reported for stratified earth with anisotropic conductivity.[4-7]
In this report, we apply the same techniques to calculate electromagnetic fields by using
an anisotropic model. We assume that both permeability and permittivity are uniaxial
with the optical axis in the z direction, perpendicular to the planes of stratification.

First, we calculate the radiation patterns produced by a horizontal electric dipole
pointing in the $\hat{x}$ direction lying on the surface of a half-space uniaxial medium. The
results indicate that in the broadside direction ($\hat{y}$ direction), the anisotropy in per-
mittivity does not affect the radiation patterns because the radiated fields are ordinary
waves with electric field vector perpendicular to $\hat{z}$.   By the same argument, radiation   JS
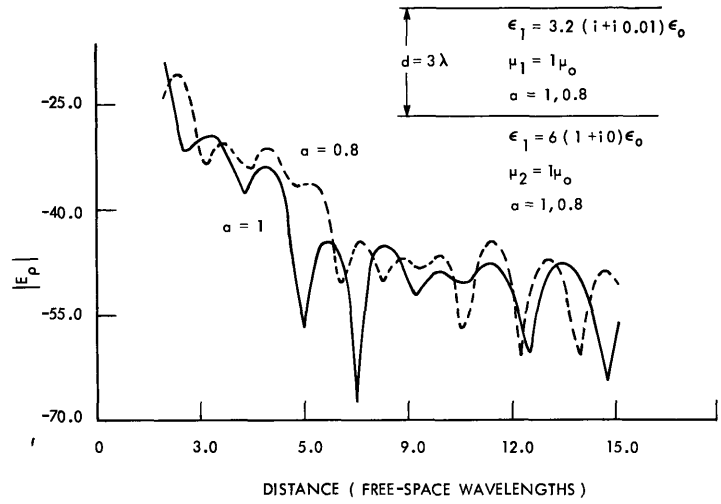
Fig. IX-5. Interference patterns for a two-layer medium with the geometric optics approach.
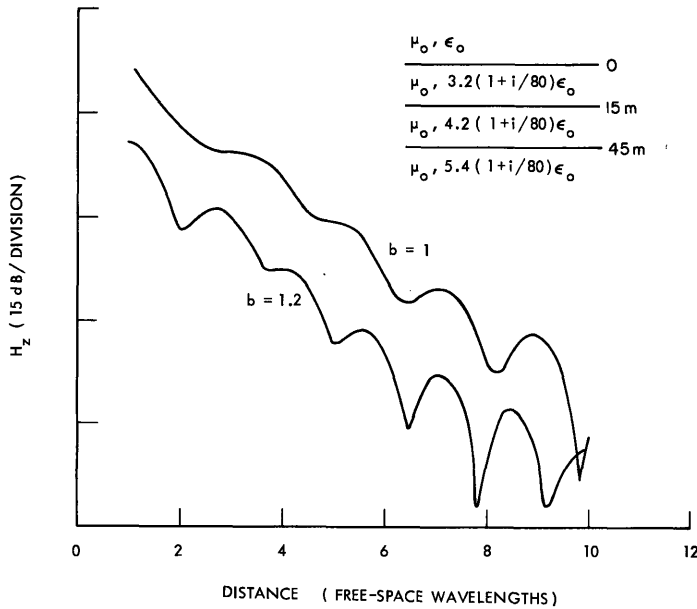

Fig. IX-6. Interference pattern for a four-layer medium using FFT.

patterns in the end-fire direction are identical to the isotropic case but not affected by the anisotropy in permeability. Using the parameters a and b to characterize uniaxial anisotropy in permittivity and permeability, we see that power couples more into the half-space medium when the medium is positive uniaxial (a > 1, b > 1). The opposite is true when the medium is negative uniaxial (a < 1, b < 1).

To illustrate the results with geometric optic and mode approaches, we treat the

case with uniaxial permittivity tensors only. We consider a slab with thickness d on top of a half space. The electric-field component in the end-fire direction, $|E_x|$, is plotted as a function of distance. In the geometric optics approach, the asymptotic field solution is calculated as

$$E_\rho = \frac{I\ell\omega\mu}{4\pi} \left\{ \frac{2}{k\rho^2} e^{ik\rho} + \frac{ak_1^2}{k^2\rho^2} \frac{\epsilon}{\epsilon_{1z}} \exp(i\sqrt{a}\,k_1\rho) \right.$$

$$\left. - \frac{i}{k^2} \sum_{m=1}^{\infty} \sqrt{a}\, k_z k_{1z}^e Y_{10} Y_{01} S_{10}^{m-1} S_{12}^m \frac{\exp(i\sqrt{a}\,k_1 R_m)}{R_m} \right\}.$$

In Fig. IX-5, we show interference patterns for $|E_\rho|$ for a = 0.8 as compared with the isotropic case for a = 1.

For thinner layers, the residue method is applied. In the case of very thin layers where no modes are excited, the contributions came from the two branch cuts and the result is

$$E_\rho = \frac{I\ell\omega\mu}{4\pi} \left\{ \frac{2}{k\rho^2} e^{ik\rho} + \frac{2k_2}{k^2\rho^2} \left(\frac{k_z Y_{01} Y_{10} \exp\left(2ik_{1z}^e d\right)}{k_{1z}^e\left(1 + S_{01}\exp\left(2ik_{1z}^e d\right)\right)^2} \right) \frac{\epsilon_{1z}}{\epsilon_{2z}} \exp(i\sqrt{a}\,k_2\rho) \right\}_{k_\rho = \sqrt{a}\,k_2}$$

For a multilayer medium, we use the fast Fourier transform (FFT) method to find the interference patterns. Figure IX-6 illustrates a four-layer stratified medium. We plot the H_z components. The permittivities are assumed to be isotropic. The layered media are all assumed to have the same anisotropic factor b. To assume fast convergence, the receiving antenna is at a height of 0.05 wavelength above ground at a frequency of 8 MHz. The result is compared with the isotropic case.

References

1. J. A. Kong, L. Tsang, and G. Simmons, "Geophysical Subsurface Probing with Radio-Frequency Interferometry" (to appear in IEEE Trans. on Antennas and Propagation).

2. L. Tsang and J. A. Kong, "Electromagnetic Fields Due to a Horizontal Electric Dipole Laid on the Surface of a Two-Layer Medium" (submitted to IEEE Trans. on Antennas and Propagation).

3. L. Tsang, R. Brown, J. A. Kong, and G. Simmons, "Numerical Evaluation of Electromagnetic Fields Due to Dipole Antennas in the Presence of Stratified Media," J. Geophys. Res. 79, 2077-2080 (1974).

4. D. N. Chetaev, "On the Field of a Low-Frequency Electric Dipole Situated on the Surface of a Uniform Anisotropic Conducting Half-Space," Sov. Phys. — Tech. Phys. 7, 991-995 (1963).

JS

5. O. Praus, "Field of an Electric Dipole above Two-Layer Anisotropic Medium," Studia Geophysica et Geodaetica (English and German translation, Prague, 1965), Vol. 9, pp. 359-380.

6. J. R. Wait, "Fields of a Horizontal Dipole over a Stratified Anisotropic Half-Space," IEEE Trans., Vol. AP-14, No. 6, pp. 790-792, November 1966.

7. A. K. Sinha and P. K. Bhattacharya, "Electric Dipole over an Anisotropic and Inhomogeneous Earth," Geophys. 32, 652-667 (1967).

JS